SUPERNOVA 1972e IN NGC 5253

Robert P. Kirshner
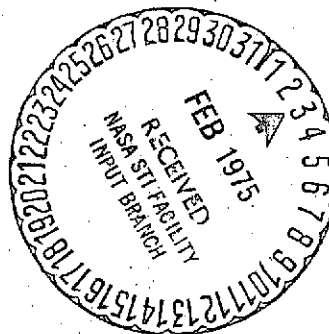
and

J. B. Oke

Hale Observatories, California Institute of Technology,
Carnegie Institution of Washington

Received _____

ABSTRACT

New absolute energy distributions of the Type I supernova 1972e in NGC 5253 extending to about 700 days after maximum light have been obtained. A physical model of the expanding envelope, based on the identification of the feature at 6550 Å with Hα, is proposed. It consists of a differentially expanding atmosphere, with electron density ranging from 10^{10} near maximum light to about 10^7, 340 days later, illuminated by a photosphere with temperature in the range 10,000°K to 7,000°K. Under these conditions, the identifications of Ca II $\lambda 8600$ and H and K, the Na D-lines and the Mg I b-lines forming P-Cygni lines are quite plausible.

More than 200 days after maximum, the spectrum is dominated by four features between 4200 Å and 5500 Å. Three of these four features match the blended emissions from over 100 lines of [Fe II]. If this identification is correct, the envelope requires about 10^{-2} $M_{\odot}$ of iron, which corresponds to an Fe/H ratio about 20 times higher than the cosmic abundance. Possible identifications of the fourth feature with Mg I $\lambda 4571$ or permitted lines of Fe II are also discussed.

Subject Headings - supernovae, stellar abundances

I. INTRODUCTION

The supernova 1972e in NGC 5253 is of special importance because its bright apparent magnitude at discovery (about B = 8 mag) (Kowal, 1972) permitted a long series of detailed investigations by numerous methods. The initial intensive series of spectrophotometry and infrared photometry conducted at the Hale Observatories has already been reported (Kirshner, Willner *et al.* 1973a, Kirshner, Oke, Penston, and Searle (KOPS), 1973b). The purpose of this paper is to report new absolute energy distributions of the supernova, covering the era 200-700 days after maximum light, and to present a general physical picture of the densities, temperatures, and abundances in the envelopes of Type I supernovae.

II. OBSERVATIONS

The observations in this paper were obtained with the multichannel spectrometer (MCSP, Oke 1969) attached to the 5-m Hale reflector. Observations were obtained over the wavelength range from 3400 Å to 10,000 Å without gaps in bands 80 Å wide shortward of 5950 Å, and 160 Å wide longward of 5950 Å. Because the supernova was always observed at large zenith distances (δ = -31°), observations of the nearby star Boss 18446 were employed to correct accurately for atmospheric extinction. The spectral energy distributions are based on the absolute calibration of α Lyrae given by Oke and Schild (1970).

One useful representation of the data is the light curve shown in figure 1, where a magnitude AB(4400) corresponding approximately to the standard B magnitude is shown. The data shown are from the spectrophotometry done at Hale Observatories only, except that pre-discovery magnitudes and upper limits are from Austin (1972). The agreement with other published photometry (Ardeberg and de Groot, 1974) is satisfactory.

The evolution of the B magnitude at early times has a simple interpretation in terms of the continuum. As shown in Kirshner *et al.* (1973a), and confirmed in the ultraviolet by Holm *et al.* (1974), smoothed scans of the supernova can be well represented by blackbodies. Table 1 gives estimates of the temperature, and the photospheric radius if the distance to NGC 5253 is 4 Mpc (Sérsic *et al.* 1972). The initial rapid decrease in B, for about 20 days, is due to the cooling of an expanding photosphere. The subsequent slower decrease in B results from the shrinkage of the photosphere at approximately constant temperature, until about JD 2441520. As shown in KOPS, after that date, the photosphere is not the principal contributor to the B-band, which is dominated by the emission bands discussed in §IV. The steady exponential decrease of flux density that sets in then is at the rate of about +0.013 mag day^{-1} for the following 640 days.

Detailed observations are shown in figure 2, which displays the log of the flux density, f_ν, versus log of the frequency, ν, on the Julian Dates listed. At the left of each scan is a tick mark, with the corresponding value of log f_ν. The mark is re-

peated at the right. Representative error bars are shown when the errors exceed 0.01 in log f_ν. Because of the large sky brightness near the horizon, and the extreme faintness of the supernova on JD 2442163 (B $\geq$ 21) only a small portion of the scan was usable.

III. CONDITIONS IN THE ATMOSPHERE

In KOPS, the similarity between the spectra of Type I and Type II supernova was used to argue that some of the same lines are present, and that the fundamental conditions under which they are formed are similar. Lines of Ca II at $\lambda 3900$ and $\lambda 8600$ were identified, along with Na I at $\lambda 5890$, and Mg I $\lambda 5174$: the P-Cygni line profiles were attributed to resonant scattering in a differentially expanding atmosphere surrounding the source of continuum emission.

In Kirshner and Kwan (1974) the photospheric velocity was inferred from the scattering profiles by determining the red edge of the absorption minimum. As indicated in table 1, this velocity has been roughly determined by scans at Ca II H and K for SN 1972e. For the dates JD 2441461 and JD 2441472, the radius of the photosphere determined from this velocity and the age is consistent with the photospheric radius

derived from the continuum flux density, the continuum temperature, and the assumed distance of 4 Mpc. In

principle, this method could be used to derive distances to Type I supernovae, (Branch and Patchett 1973) however a great deal of continuum information is required to make a reasonable estimate of the photospheric temperature.

In KOPS, the possible identification of Balmer lines is discussed. During the first week of observation, there is no clear sign of any of the Balmer lines, except for a broad blend extending from the wavelength of Hα about 300 Å to the blue. However, beginning on JD 2441460, a strong emission feature emerges from that blend at the wavelength of Hα, and by JD 2441484, that feature dominates the region of the spectrum from 6200 Å to 6700 Å. At about the same time, an emission feature appears at the wavelength of Hγ. Near Hβ, the spectrum is too complex and blended to be certain whether Hβ is present or not.

Although some doubt lingers about the correctness of the identification, and it is difficult to estimate the correct level of the continuum, the total Hα photon flux, and the corresponding electron density are listed in table 2.

Despite the relative weakness of the hydrogen features, the electron densities (10^{10}-10^7 cm^{-3}) and the mass of ionized matter (about 0.1 M_Θ) are only a little smaller than the corresponding numbers derived by Kirshner and Kwan (1975) for Type II supernovae.

As shown for SN II's, the recombination time is short compared to the age of the supernova. The photospheric flux of ionizing photons beyond the Balmer limit is somewhat larger than the recombination rate in the first two months of observation,

and comparable to it at later times. As for SN II's, it is possible for photoionization from the $n = 2$ level to replenish the electron supply and maintain the electron density at the observed levels. This mechanism can operate only if there is sufficient opacity in Lyman α to prevent its rapid escape. About 1 $M_\odot$ of hydrogen is required to slow the escape rate so that the photospheric ionizing flux can maintain the ionization. This rough estimate of the hydrogen mass in the envelope will be used to estimate the relative abundances of other elements.

The similar electron densities, temperatures, and dynamics of SN I's and SN II's helps account for some of the similarities in their spectra. The differences may arise from an unusually high relative abundance of elements heavier than hydrogen. In that case, the strong and numerous lines of SN I's might be due to more line-forming ions relative to the continuum-forming hydrogen and electrons. If Type I supernovae arise from evolved stars, or if nucleosynthesis takes place during the explosion, such an enriched envelope is not an unlikely possibility.

IV. LATE PHASE

A. Strong Emission Features

When the scans of SN 1972e made after JD 2441684 are compared with those made during the first 70 days of observations (KOPS), some important changes are apparent.

The most significant change is that the continuum ceases to be the dominant feature, although it still appears to be present. The emissions at $\lambda\lambda 5300$, 5000, 4200 and especially at 4600 have become the outstanding features. Because the continuum lies so far below these features, it is most unlikely that they are formed by scattering photospheric photons. Indeed, the Ca II lines at H and K and at $\lambda 8600$, and the Na I D-lines have emission peaks which lie so far below the strong emissions that the absorptions are the conspicuous features. The continued presence of these absorptions is the best evidence for the persistence of the continuum. By JD 2441865, the Ca II absorptions can scarcely be distinguished from the noise.

The strong emission lines have some unusual properties which offer insight into their possible identifications. First, the decrease in flux from the blend is exponential in time over the _entire_ range of observations, going back to the earliest days. Second, the relative strengths of the lines in the blend change very little, despite significant changes in electron density and temperature.   Third, almost all the emission observed at late times is concentrated in the blend from $\lambda\lambda 4000-5500$.

Table 3 lists the observed flux from each of the four components of the blend after subtracting an estimated continuum, and the corresponding photon emission rate if NGC 5253 is at a distance of 4 Mpc. During the first 70 days of observations (JD 2441453-2441529), the overall photometric behavior of the supernova depends on the cooling and then shrinking photosphere. From JD 2441653-2442163, the exponential decay of the emission blend determines the B-magnitude. However, over the entire period of observation the flux, $F(\text{erg s}^{-1})$, in the blend alone appears to be exponential. A good approximation is:

$$\log F = -0.55 \ (t/10^7 s) + 41.6 \tag{1}$$

Thus the clear emergence of these lines at age near 200 days is a result of the more rapid decay of continuum flux.

The relative fluxes in the four lines are roughly constant, as table 3 demonstrates. The fraction of the total flux from the blend that comes from the $\lambda 4600$ line is large, and roughly constant. This suggests that all four lines respond in nearly the same way to the changes in density and temperature taking place in the expanding envelope. This could happen if all the lines were due to the same ion, and arose from about the same excitation potential. Alternatively, it might result if the lines come from atoms or ions of similar ionization potential, comparable energy level differences, and the same dependence of photon production on electron density.

B. Mechanisms for Line Production

When the continuum is weak compared to the strong emission features, some mechanism other than resonant scattering is required to produce the lines. In this section, general arguments are advanced to show that collisions can provide the needed excitation, and that the observed lines are likely to have low Einstein A's.

Emission lines can be formed through recombination. At late times, the continuum flux lies far below the line emission, so that each net recombination destroys the ion and very few compensating photoionizations take place.

The strong blend of lines between $\lambda\lambda 4000-5500$ persists for over 200 days, emitting a total of roughly 10^{59} photons. If the lines were formed by recombination, this would require about 10^{59} ions. Even if they were protons, this would imply 100 $M_{\odot}$. Since they are surely more massive, the total mass would be intolerably high. For this reason, recombination cannot be responsible for the observed emission.

Collisional excitation can be considerably more efficient and, if it is responsible for the emission, the variation of the emission with changing density and temperature gives direct evidence on the type of transition that produces the observed lines. In particular if the line has a large Einstein A compared to the downward collision rate, $n_e \gamma$, every upward collision produces a photon. Then the rate at which photons are produced from a given mass of target atoms, Q, is propor-

tional to $n_e T^{-1/2} \exp(-E/kT)$. We expect $H = QT^{1/2} \exp(E/kT) n_e^{-1}$ to remain constant despite variations in Q, n_e and T, if the line has $A \gtrsim n_e \gamma$. Here H is the ratio of photons observed each second to the expected rate of production for the case of high Einstein A.

On the other hand, if the line has a low Einstein $A \lesssim n_e \gamma$, collisions establish the ratio between the upper and the lower levels at the Boltzmann ratio for the electron temperature independent of the density. For such a thermalized transition we can define L as the ratio of photons observed to the number expected and we would expect $L = Q \exp(E/kT)$ to remain constant.

In table 4, the evidence is presented: normalized values of H and L are calculated using E corresponding to 5000 Å, the photospheric temperature at early times and 5000°K at late times, values of n_e from table 2, and values of Q from table 3. It is quite apparent from table 4 that L is much more nearly constant than H over a large range of Q, n_e, and T. Thus the circumstantial evidence favors lines with low $A/n_e \gamma$ as the source of the strong emission features. At the temperatures of interest, de-excitation rates for forbidden lines are typically of order $\gamma = 10^{-7}$, so for $n_e \gtrsim 10^7$, we require $A \lesssim 1 \ s^{-1}$. If forbidden lines are the source of the strong emission features, the larger flux observed at early times is due to the higher temperature and not to the increased density. A linear decrease of the electron temperature with time would produce the exponential decay of the flux in the blend that is seen in equation (1).

C. Specific Possibilities

We conducted a search among the more abundant elements for forbidden lines which might contribute to the strong emission blend without producing other lines which are not observed. Possible atoms and ions expected in the moderate density and weak photoionization field of an expanding supernova envelope are: He I, C I, N I, O I, Ne I, Mg I, Si I, S I, Ar I, and Fe II. Of these, the only lines arising from the ground state that might contribute to the broad emission blend are N I ($\lambda\lambda 5200$, 5198), Mg I ($\lambda 4571$), S I ($\lambda 4589$), and numerous forbidden lines of Fe II. Chief among the iron lines are the multiplets $\lambda\lambda 4287$, 4359 (7F), 4416 (16F), 5159 (19F), 4815 (20F) and 4244, 4277 (21F).

The nitrogen lines have very small Einstein A's: about 1.6×10^{-5} for $\lambda5198$, and 7×10^{-6} for $\lambda5200$ (Garstang, 1956). At electron densities of 10^7, the population in the upper state depends only on T_e, and the emission rate, Q, is independent of n_e. At 5000°K, the expected emission in the $\lambda5200$ line is about 2×10^7 N(N I) photon s^{-1}. With a typical observed flux of 2.5×10^{51} photon s^{-1} in the $\lambda5200$ component of the emission blend, 1.1×10^{58} N I atoms would be required. Since this would imply 125 $M_\odot$ of N I alone, we may safely disregard N I as the source for this emission.

The S I line is an unlikely identification, because the $\lambda4589$ line and the $\lambda7726$ line share the same upper state and have Einstein A's in the ratio 1:5. If S I were an important contributor to the $\lambda4600$ feature, we would expect a feature at $\lambda7726$ with five times as many photons. Although some emission is observed near $\lambda7700$, it is nowhere near the required strength.

The $\lambda4571$ line of Mg I is an intersystem transition, connecting the $^3P_2$ upper state with the $^1S_0$ ground state. The Einstein A for the transition is somewhat uncertain, but is of

order 400 (Wiese *et al.* 1969). Thus, when the electron density drops below about 10^9, the photon emission rate is set by the electron collision rate. Although this is at variance with the argument from table 4, the results are very interesting. Very roughly, if γ = 1, then each Mg I atom produces 7×10^{-3} photon s^{-1} at n_e = 3×10^7 and T = 5000°K. On JD 2441684, about 4×10^{51} photon s^{-1} are observed, which requires about 6×10^{53} Mg atoms. One solar mass at cosmic abundance contains about 3×10^{52} Mg atoms. Three possible conclusions might be drawn from this: that the λ4600 line is not formed by Mg I, or that the abundance of Mg is enhanced, or that the physical conditions and atomic parameters are not well enough known to decide. Because of the sensitivity of the result to the electron density and temperature, no firm conclusion seems warranted, however it is tempting to speculate that collisional excitation of Mg I might contribute to the λ4600 component of the strong emission blend.

An examination of the multiplet table (Moore 1945) listing for [Fe II] reveals no less than 216 forbidden lines arising either from the ^6D ground state of the ^4F state 0.3 eV above it. Fortunately, the Einstein A for every one of these lines has been calculated by Garstang (1962). None of the A's is bigger than about 1 s^{-1}, so electron densities of 10^7 or greater will ensure that the upper states are populated to the Boltzmann level. In that case, the photon flux contributed by each line is proportional to (2J (upper) + 1) A exp(-E/kT), and the total photon flux is just the sum over all the contributing terms.

The quantity (2J+1)A was calculated for each of the 105 lines with A > 0.01, and the sum for every 100 Å interval from $\lambda 3000$ to $\lambda 10000$ was computed, and weighted by $\exp(-E/kT)$, with T = 5000°K. The bottom tracing of figure 2 shows the logarithm of the sum, which should be proportional to the log of the photon flux in each band. The only region over the entire wavelength range with any significant emission is the interval from $\lambda\lambda 4200$-5500. Furthermore, there is a very good agreement between the relative strengths of the three blends of [Fe II] predicted by this calculation and the observed features at $\lambda 5200$, $\lambda 4800$, and $\lambda 4300$. Even the small bump on the long wavelength side of the $\lambda 5200$ peak near $\lambda 5500$ is reproduced. Only the feature at $\lambda 4600$ is not predicted.

Figure 2 includes all the strong lines between $\lambda 3000$ and $\lambda 10000$ that would be produced by [Fe II] at low temperature, and a density of 10^7 or more. The next strongest feature, a blend at $\lambda 3300$, would be an order of magnitude weaker than the blends shown in the figure. Of course, more than a demonstration of possible wavelength coincidences is needed before we can be confident that the lines of [Fe II] account for three of the four strong features that dominate the late spectra of Type I supernovae. We also require that the photon flux be produced under the observed conditions. Since for Boltzmann conditions we have:

$$\frac{n_u}{n_\ell} = \frac{g_u}{g_\ell} e^{-E/kT} \quad . \tag{2}$$

Then the photon flux summed over all the [Fe II] lines is given by:

$$Q([Fe\ II]) = \int (\sum n_u A) dV = (\sum g_u A) \frac{e^{-E/kT}}{g_\ell} \int n_\ell dV \quad . \tag{3}$$

Putting in the appropriate values, we can write the total number of iron ions required to produce the observed photons.

$$N(Fe\ II) = \int n_\ell dV = \frac{Q(Fe\ II)\ g_\ell e^{E/kT}}{\sum g_u A} =$$

$$Q(Fe\ II)\ 0.27\ \exp\left(\frac{2.88\ \times\ 10^4}{T}\right) \quad . \tag{4}$$

Using the photospheric temperatures through the early times when they are fairly well known, and T = 5000°K for the late times when they are not, N(Fe II) has been tabulated for each time in table 5. It shows that the required amounts of iron are modest in terms of the total mass, but that the required abundance relative to hydrogen is rather high: about 20 times higher than usually regarded as the cosmic abundance (Cameron 1973). This abundance estimate is considerably more reliable than in the

the case of Mg I, because the dependence on physical conditions is weak, and the atomic data reasonably well known. In the context of Type I supernovae, such large iron abundance is made plausible by the possibility that the exploding star is a highly evolved object, and that explosive nucleosynthesis may take place during the supernova event.

The production of about 10^{-2} $M_\odot$ of Fe in a supernova does not lead to an excessive mass of iron in the galaxy. If, in 10^{10} years, there are 10^8 SN I's, about 10^6 $M_\odot$ of Fe will be ejected. If the mass of our galaxy is 10^{11} $M_\odot$, the observed iron abundance of 10^{-3} by mass far exceeds the 10^6 $M_\odot$ produced by SN I's at the current rate.

What are the other observable consequences of such a high iron abundance? In KOPS, scans show that at early times $\lambda 4600$ and $\lambda 5000$ had strong P Cygni features which were ascribed to resonant scattering from the very same metastable levels that form the upper states of the forbidden lines. For SN II's the optical depths of these lines were quite large with normal iron abundance, for SN I's, they should be considerably larger. It is possible that at early times, when the continuum is strong, these lines are the features at $\lambda 4600$ and $\lambda 5000$, and that the forbidden lines are not important contributors.

In that case, the first two or three entries in tables 3 and 4 may be irrelevant: the lines are formed by scattering and not by collisions. If that is so, then the late evolution of

Q(Fe II) in table 4 is just as reasonably described by the high $A/\gamma n_e$ model as by the low $A/\lambda n_e$ model. Is it possible that collisions produce the $\lambda 4600$ feature at late times? The $\lambda 4600$ feature would be due to the strong lines of multiplets 37 and 38. We can estimate whether this could possibly produce the observed emission. From Allen (1963), multiplet 38 has a collisional excitation rate (at 5000°K) of about $\gamma(up) = 2 \times 10^{-8}$ s^{-1}. On JD 2441653 when $n_e = 4.4 \times 10^7$, $\gamma(up)n_e \simeq 1$ s^{-1}. The Boltzmann population in the lower state of multiplet 38 is about 2×10^{-3} of the ground state, so if the total iron number is 5×10^{53}, as inferred from the forbidden lines we expect about 1×10^{51} ions in that state. Thus we expect about 1×10^{51} photons s^{-1} to be produced in this way. A similar contribution from multiplet 37 raises the expected photon flux to 2×10^{51} s^{-1}. The observed amount is about 9×10^{51}. Since the electron density, temperature, and total iron number are not well known, it may well be that the $\lambda 4600$ feature in emission at late times is also due to collisional excitation of permitted Fe II.

In the same way the lines of multiplet 42 may contribute at 5000 Å, while other possible features are multiplets 27(4233, 4351) and 28(4179, 4297).

Overall, the case for Fe II lines both forbidden and permitted as the main source of the strong emission features seen at late stages of SN I's seems plausible. More detailed investigation may be able to confirm or deny this interpretation.

D. [O I] Emission

As indicated in KOPS, the evolution of the energy distributions of Type I supernovae is very similar from one individual case to the next. In particular, the agreement between the spectra of 1937c in IC 4182 (Minkowski 1937, Greenstein and Minkowski 1973) and the scans of 1972e in NGC 5253 is detailed. One feature observed by Minkowski that is not present in the scans of figure 2 is the [O I] emission at $\lambda6300, 6363$. Minkowski observed those lines after the 184th day past maximum. Although he found their appearance, in the absence of other familiar nebular lines, to be quite remarkable, Minkowski was confident that the observed features were not due to [O I] emission from the airglow. In the last scan of figure 2, more than 400 days after maximum, the upper limit on the [O I] flux corresponds to the emission at 5000°K from 0.25 $M_{\odot}$ of gas with high $n_e\gamma/A$ and normal oxygen abundance. Thus, the failure to detect these lines does not lead to any serious contradiction with the assumption of about 1 $M_{\odot}$ of gas, although it does seem to indicate that the oxygen abundance relative to hydrogen cannot be very greatly enhanced.

It is possible that the finer resolution of Minkowski's spectra permitted him to detect fainter emission features when they were narrow, but it is still surprising that they were undetected in the scans at age 400 days.

E. The Energy Crisis

The most difficult problem in understanding the emission during the late phases of supernovae is the source of energy. This is a problem whatever the details of the emission mechanism; for collisional excitation it takes the form of keeping the electrons hot. Photospheric heating is inadequate, and the thermal energy of the gas itself would only last for about 10^4 s. Only a small fraction (10^{-3}) of the mechanical energy in the expansion of the gas is needed to heat the electrons, but it is not clear how this might come about. When the energy source is understood, some real understanding of supernova emission will have been attained.

REFERENCES

Allen, C. W. 1963, *Astrophys. Quantities* (London: The Athlone
Press).

Branch, D. and Patchett, B. 1973, *M.N.R.A.S.* 161, 71.

Cameron, A. G. W. 1973, in *Explosive Nucleosynthesis*, eds. D.
N. Schramm and W. D. Arnett (Austin: University of Texas
Press), page 3.

Garstang, R. H. 1956, in *The Airglow and the Aurora*, eds. E. B.
Armstrong and A. Dalgarno (New York: Pergamon Press), page
324.

Garstang, R. H. 1962, *M.N.R.A.S.* 124, 321.

Greenstein, J. L. and Minkowski, P. 1973, *Astrophys. J.* 182, 225.

Holm, A. V., Wu, C. C., and Caldwell, J. 1974, *Publ. Astron. Soc.
Pacific* 86, 296.

Kirshner, R. P., Oke, J. B., Penston, M. and Searle, L. 1973a,
Astrophys. J. 185, 303.

Kirshner, R. P., Willner, S. P., Becklin, E. E., Neugebauer, G.,
and Oke, J. B. 1973b, *Astrophys. J. Letters* 180, L97.

Kirshner, R. P. and Kwan, J. 1974, *Astrophys. J.* 193, 27.

Kirshner, R. P. and Kwan, J. 1975, *Astrophys. J.* in press.

Kowal, C. T. 1972, *I.A.U. Circ.* No. 2405.

Lee, T. A., Wamsteker, W., Wishniewski, W. Z., and Wdowiak, T.
J. 1972, *Astrophys. J. Letters* 177, L59.

Minkowski, R. 1939, *Astrophys. J.* 89, 143.

Moore, C. 1945, *A Multiplet Table of Astrophysical Interest* (re-
vised ed.), Princeton University Observatory Contributions,
No. 20.

Morrison, P. and Sartori, L. 1969, *Astrophys. J.* 158, 541.

Oke, J. B. and Schild, R. E. 1970, *Astrophys. J.* 161, 1015.

Sérsic, J. L., Carranza, G. and Pastoriza, M. 1972, *Astrophys. Sp. Sci.* 19, 469.

Wiese, W. L., Smith, M. W., and Miles, B. M. 1969, *Atomic Transition Probabilities*, NBS-22, Gov't. Printing Office, Washington D. C.

FIGURE CAPTIONS

Figure 1   AB(4400) versus Julian Date for SN 1972e.

AB(4400) = -2.5 log f_ν -48.60, and corresponds

roughly to B −0.2, where B is the standard B

magnitude.

Figure 2   Energy distributions for SN 1972e, with log f_ν

versus log ν. Julian Dates and log f_ν values

are indicated for each scan. Representative

error bars are shown in the scans and spectral

regions where they are significant, except for

JD 2442163, about 700 days after maximum, when

all error bars are shown. The bottom scan

represents the relative photon emission from

[Fe II] at T = 5000°K, with n_e greater than about

10^7, as described in the text.

TABLE 1

Photospheric Behavior of SN 1972e in NGC 5253

Date	JD-2440000	T (°K)	r(ph) (cm)	v(ph) (cm s^{-1})	t (s)	vt (cm)
1972 May 24	1461	10000	1.1+15	1.4+9	7.8+5	1.1+15
1972 June 4	1472	7500	1.6+15	1.1+9	1.7+6	1.9+15
1972 June 15	1483	7000	1.1+15	1.0+9	2.7+6	2.7+15
1972 June 25	1493	7000	1.0+15	1.0+9	3.5+6	3.5+15

TABLE 2

Hydrogen Recombination

JD-2440000	$f(H\alpha)$ (erg cm^{-2}s^{-1})	$Q(H\alpha)$	$R(atm)$ (cm)	V_3 (cm^3)	$\alpha(T)$	n_e	$M_\odot$ (H^+)
1453	(4-11)	2+52	(8+14)	2+45	2-14	2+10	4-2
1460	(2-11)	1+52	(1.1+15)	6+45	2-14	1+10	5-2
1472	1-10	6+52	(1.6+15)	2+46	3-14	1+10	1-1
1484	3-11	2+52	(1.7+15)	2+46	4-14	5+9	7-2
1493	2-11	1+52	(1.8+15)	2+46	4-14	4+9	7-2
1504	2-11	1+52	(2.3+15)	5+46	5-14	2+9	9-2
1507	1-11	6+51	(2.4+15)	6+46	5-14	2+9	7-2
1529	5-12	3+51	(3.4+15)	2+47	5-14	6+8	8-2
1653	4-13	3+50	(8.5+15)	3+48	5-14	4+7	9-2
1684	2-13	1+50	(1.0+16)	4+48	5-14	3+7	8-2
1796	7-14	4+49	(1.5+16)	1+49	5-14	8+6	9-2

TABLE 3

Flux From Members of the Strong Blend

JD-2440000	1453	1469	1529	1653	1684	1796	1865	2163
$t/10^7$(s)	.017	0.16	0.67	1.75	2.01	2.98	3.50	6.15
f(5200) (erg-cm^{-2}-s^{-1})	----	8-11	2-11	8-12	4-12	8-13	3-13	----
f(5000)	----	6-11	3-12	3-12	2-12	5-13	2-13	3-14
f(4600)	<2-10	7-11	2-11	2-11	1-11	2-12	6-13	4-14
f(4200)	----	----	<1-12	4-12	2-12	5-13	4-13	3-14
f(4600)/ Σf	----	0.30	0.49	0.54	0.56	0.53	0.44	0.41
ΣF (erg s^{-1})	<5+41	4+41	9+40	6+40	3+40	7+39	3+39	2+38
ΣQ (photon/s)	<1+53	9+52	2+52	1+52	8+51	2+51	6+50	4+49

TABLE 4

Line Variation Mechanisms

JD-2440000	H (normalized)	L (normalized)
1453	<0.24	<0.7
1469	1.0	1.0
1529	8	0.3
1653	40	1.3
1684	400	1.0
1796	250	1.6

TABLE 5

Required Mass of Ionized Iron

JD- 2440000	Q([Fe II])	N(Fe II)	$M_{\odot}$(Fe II)
1453	<1+53	<5+53	2-2
1469	.6+52	6+53	3-2
1529	1+52	2+53	8-3
1653	6+51	5+53	2-2
1684	4+51	3+53	1-2
1796	8+50	6+52	3-3

NGC 5253
1972 e

NGC 5253
1972 e

2441684

2441796

2441865

2442163

[Fe II]

Ca II   α   Na I   Mg I β   γ   Ca II